PCCP

Adsorption and photochemistry of CH_3CN and CH_3CONH_2 on powdered TiO_2

Chih-Chung Chuang, Wen-Chun Wu, Ming-Xi Lee and Jong-Liang Lin*

Department of Chemistry, National Cheng Kung University, 1, Ta Hsueh Road, Tainan, Taiwan, 701, ROC. E-mail: jonglin@mail.ncku.edu.tw

Received 24th April 2000, Accepted 4th July 2000
Published on the Web 1st August 2000

The adsorption and photochemistry of acetonitrile and acetamide on TiO_2 have been studied by Fourier-transform infrared spectroscopy (FTIR). Adsorbed CH_3CN, CH_3CONH_2, η^2(N,O)-CH_3CONH are formed after CH_3CN adsorption on TiO_2. The last two species are due to surface hydroxy groups attacking the electron-deficient carbon in the cyano group of the adsorbed acetonitrile. UV exposure causes decomposition of CH_3CN(a) to CH_2CN(a) and decomposition of CH_3CONH_2(a) and η^2(N,O)-CH_3CONH(a) to CH_3COO(a), HCOO(a), NCO(a) and CN-containing species on the surface.

Introduction

Due to the sensitive variation in the CN stretching frequency of CH_3CN bonded on various surface sites, it has been used to probe the surface states of metals and metal oxides. CH_3CN is bonded to Pt(111) by η^2(C,N) coordination at sub-monolayer coverage, *i.e.*, C and N atoms are coordinated simultaneously to the surface. At this bonding geometry, the C=N stretching absorbs at 1615 cm^{-1}, as evidenced by electron energy-loss spectroscopy (EELS).[1] On Ni(111), Sexton[1] and Kishi[2] have proposed that CH_3CN is also adsorbed with η^2(C,N) coordination in contrast to the bonding geometry through the N atom proposed by Friend *et al.*[3] On Ag(110), CH_3CN is weakly adsorbed on the surface and is desorbed at 166 K. However, on a partially oxidized Ag surface, CH_3CN is more strongly adsorbed with the CN π-electrons interacting with surface Lewis acid sites, exhibiting CN stretching at 1840 cm^{-1}.[4] Further EELS study shows the formation of a CH_2CN anionic adsorbed species with a 2075 cm^{-1} CN stretching frequency, indicating the Brønsted base character of the partially oxidized Ag surface.[4] On metal oxides, based on the extent of the blue-shift of the CN stretching of CH_3CN coordinated through the N atom to surface Lewis or Brønsted acid sites, the relative acidity of the sites can be measured.[5–12] In addition to the acid–base interaction, CH_3CN may dissociate on some metal oxides. On α-Fe_2O_3, CH_3CONH_2(a) and CH_3CONH(a) are formed from the reaction of CH_3CN and surface OH groups.[13] CH_3CONH(a) is also observed on ZnO[14] and δ-Al_2O_3[15] and can be chemically transformed into CH_3COO(a). CH_3CN on CeO_2 forms anionic CH_2CN and CH_3CNO species.[16] Photocatalyzed oxidative degradation of CH_3CN on TiO_2 has been studied by Lichtin *et al.*[17] and by Zhuang *et al.*[18] Lichtin's group observed, by gas chromatography, the formation of a $(CN)_2$ intermediate and CO_2, H_2O and HNO_3 products. Zhuang *et al.* found, using IR spectroscopy, the isocyanate species (NCO) adsorbed on the surface during CH_3CN photooxidation. From the product distribution of CH_3CN photodegradation on TiO_2, multiple reaction routes must occur. For example, $(CN)_2$ and NCO from C–C bond cleavage, HNO_3 from C≡N triple bond cleavage and H_2O from C–H bond cleavage are expected. Considering the complex chemical behavior, it is worth further study of CH_3CN photooxidation to gain more insights into the reaction pathways.

In the present paper, in addition to the study of photooxidation of CH_3CN on TiO_2 in relation to the issue of photooxidative destruction of organic molecules detrimental to the environment, we focus on the interaction of CH_3CN with surface hydroxy groups present on the TiO_2 surface; it is found that CH_3CONH_2 and CH_3CONH are generated on the surface. Therefore the adsorption and photochemistry of CH_3CONH_2 are also investigated.

Experimental

The preparation of TiO_2 powder supported on a tungsten fine mesh (~6 cm^2) has been described previously.[19,20] Briefly, TiO_2 powder (Degussa P25, ~50 m^2 g^{-1}, anatase 70%, rutile 30%) was dispersed in water–acetone solution to form a uniform mixture which was then sprayed onto a tungsten mesh. The TiO_2 sample was then mounted inside the IR cell for simultaneous photochemistry and FTIR. The IR cell with two CaF_2 windows for IR transmission down to 1000 cm^{-1} was connected to a gas manifold which was pumped by a 60 L s^{-1} turbomolecular pump with a base pressure of ~1×10^{-7} Torr. The TiO_2 sample in the cell was heated to 450 °C under vacuum for 24 h by resistive heating. The temperature of the TiO_2 sample was measured by a K-type thermocouple spot-welded onto the tungsten mesh. Before each experimental run, the TiO_2 sample was heated to 450 °C in vacuum for 2 h. 10 Torr O_2 was then introduced into the cell as the sample was cooled to 70 °C. When the TiO_2 temperature reached 35 °C, the cell was evacuated prior to gas dosing. The TiO_2 surface after the above treatment still possessed residual hydroxy groups.[21] Before introducing the vapor to the cell, CH_3CN (liquid, 99.97%, Tedia) was purified by several freeze–pump–thaw cycles; CH_3CONH_2 (solid, 98%, Aldrich) was well-outgassed under vacuum. O_2 (99.998%) was used as received from Matheson. The pressure was monitored with a Baratron capacitance manometer and an ion gauge. In the photochemistry study, both the UV and IR beams were set 45° to the normal of the TiO_2 sample. The UV light source used was a combination of a 350 W Hg arc lamp (Oriel Corp), a water filter, and a band pass filter with a band width of ~100 nm centered at 320 nm (Oriel 51650). The power at the position of the TiO_2 sample was ~0.24 W cm^{-2} measured in the air by a power meter (Molectron, PM10V1). CH_3CN and CH_3CONH_2 are transparent for the wavelength used in this

study.[22] IR spectra were obtained with 4 cm^{-1} resolution using a Bruker FTIR spectrometer with a MCT detector. The entire optical path was purged with CO_2-free dry air. The spectra presented here have been ratioed against a clean TiO_2 spectrum providing the background reference.

Results and discussion

Adsorption of CH_3CN and CH_3CONH_2

Fig. 1(a) shows the IR spectra of TiO_2 exposed to 2 Torr of CH_3CN and then evacuated at 35 °C. The absorptions in the 3600–3800 cm^{-1} region due to isolated surface hydroxy groups are attenuated following CH_3CN adsorption. Bands located at 1367, 1415, 1433, 1469, 1537, 1578, 1630, 2279, 2289, 2308, 2315, 2937 and 2998 cm^{-1} are observed. Table 1 compares our observations with the IR absorptions of CH_3CN molecules in the liquid and solid states (first two columns of Table 1) and CH_3CN on TiO_2 at 200 K (third column, Table 1) reported by Zhuang *et al.*[18] The CN stretching frequency of adsorbed CH_3CN is affected by its adsorption sites on TiO_2 as shown in the fourth column in Table 1. Absorptions in the region 1250–1750 cm^{-1} are more complex, to clearly assign the bands in this range, CD_3CN adsorption on a TiO_2 surface has also been studied. Prior to CD_3CN dosing into the reaction cell, the OH groups on TiO_2 were replaced with OD(a) by repeating several cycles of D_2O adsorption, annealing, and evacuation at 250 °C until no OH(a) was found. Fig. 1(b) shows the IR spectrum of TiO_2 exposed to 2 Torr of CD_3CN and then evacuated at 35 °C. Following CD_3CN adsorption, as in the CH_3CN case, attenuation of OD(a) absorptions in the region 2650–2800 cm^{-1} is also observed (not shown). In the CN stretching frequency range, a strong, broad band peaked at 2297 cm^{-1} and two small bands at 2217 and 2252 cm^{-1} appear. It is noteworthy that Fermi-resonance of CN stretching is absent in the CD_3CN case. The unresolved, strong band at 2297 cm^{-1} can be assigned to the CN stretching mode of CH_3CN(a) interacting with surface OD groups and Lewis acid sites. Its high intensity indicates that most of the adsorbed CD_3CN molecules adopt such surface adsorption states. The weak band located at 2252 cm^{-1} is the same as or very close to the CN stretching absorption of liquid or solid CH_3CN molecules[23] and can be attributed to a small amount of physisorbed CD_3CN on the surface. The other weak 2217 cm^{-1} band is similar to the previously observed band at 2211 cm^{-1} for CD_3CN in the solution phase, which has been ascribed to the overtone of CD_3 symmetric bending.[24] For the absorptions in the 1250–1750 cm^{-1} region, bands at 1416, 1435, 1465, 1518 and 1622 cm^{-1} are observed. All these bands have similar frequencies, but with varying intensity relative to CH_3CN absorptions in this range. However, no strong, sharp band at ~1367 cm^{-1} is observed in Fig. 1(b), therefore this peak is assigned to CH_3 symmetric bending of CH_3CN. Table 1 summarizes the band assignment for the CH_3CN vibrational frequencies observed after the adsorption of CH_3CN and CD_3CN on TiO_2. The bands in the region 1250–1750 cm^{-1} in Fig. 1, except that at 1367 cm^{-1}, cannot be completely attributed to the adsorbed acetonitrile, because they are observed for both CH_3CN and CD_3CN compounds. The lack of an isotope shift indicates that some of the CH_3CN and CD_3CN have, after adsorption on TiO_2, been chemically transformed into other species on the surface. Previously, Lorenzelli *et al.*[13] investigated CH_3CN adsorption on α-Fe_2O_3 and found absorption bands at 1380, 1450, 1470, 1560 and 1640 cm^{-1} which could not be attributed to adsorbed CH_3CN. Furthermore, a similar absorption feature was obtained after adsorption of CH_3CONH_2 on this surface. Accordingly, the above five bands observed in CH_3CN adsorption on α-Fe_2O_3 were

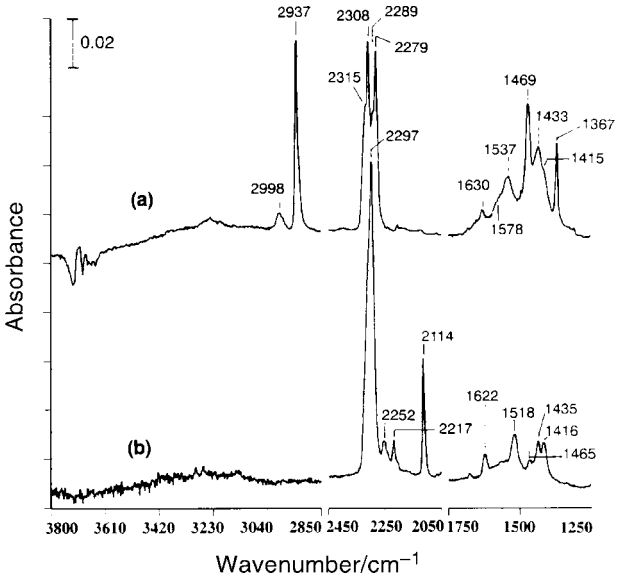

Fig. 1 IR spectra of a TiO_2 surface exposed to 2 Torr of CH_3CN (a) and CD_3CN (b) at 35 °C and then evacuated for 20 min. Both spectra were recorded with 50 scans at 35 °C. The mass of TiO_2 used was ~70 mg.

Table 1 Comparison and assignments for the vibrational frequencies of acetonitrile

CH_3CN						
Liquid (ref. 23)	Solid (ref. 23)	CH_3CN/TiO_2 200 K (ref. 18)	Mode description	CH_3CN/TiO_2 (this work)	CD_3CN/TiO_2 (this work)	Mode description
3001	3000	3001	$\nu_a(CH_3)$, CH_3CN	2998		
2942	2936	2939	$\nu_s(CH_3)$, CH_3CN	2937	2114	$\nu_s(CD_3)$, CD_3CN
		2318	$\nu(C{\equiv}N)$, $Ti{\cdots}N{\equiv}CCH_3$	2315		
2293	2293	2298	[$\nu(C{\equiv}N)$, Fermi-resonance and $\delta_s(CH_3) + \nu(C{-}C)$	2308		[$\nu(C{\equiv}N)$.
				2289	2297	$Ti{\cdots}N{\equiv}CCD_3$
		2274	$\nu(C{\equiv}N)$, $Ti{-}OH{\cdots}N{\equiv}CCH_3$	2279		$Ti{-}OD{\cdots}N{\equiv}CCD_3$
2252	2248		$\nu(C{\equiv}N)$, CH_3CN		2252	$\nu(C{\equiv}N)$, physisorbed CD_3CN
					2217	$2\delta_s(CD_3)$, CD_3CN
				1630	1622	
				1578		
				1537	1518	
				1469	1465	
				1433	1435	
1415	1420–36	1414, 1444	$\delta_a(CH_3)$, CH_3CN	1415	1416	
1368–70	1366–70	1367	$\delta_s(CH_3)$, CH_3CN	1367		

attributed to the generation of CH_3CONH_2(a) responsible for the 1380, 1470 and 1640 cm^{-1} and its dissociative adsorption species, CH_3CONH(a), responsible for 1450 and 1560 cm^{-1} due to –CNO– stretching vibrations. Krietenbrink *et al.*[15] have observed similar chemical transformation of CH_3CN into CH_3CONH(a), evidenced by bands at 1495 and 1595 cm^{-1}, on δ-Al_2O_3. In the present study, the bands at 1415, 1433, 1469, 1537, 1578 and 1630 cm^{-1} observed after CH_3CN adsorption on TiO_2 (see Fig. 1(a)) are very likely due to CH_3CONH_2(a) and CH_3CONH(a) formation. The bands due to C=O and C–N stretching vibrations of CH_3CONH_2(a) and those due to –CNO– stretching vibrations of CH_3CONH(a) would not show a primary isotope shift as H is replaced by D. This explains, except for the CH_3 symmetric bending at 1367 cm^{-1} in the CH_3CN case, why similar absorption frequencies in the 1250–1750 cm^{-1} range are detected after CD_3CN and CH_3CN adsorption on TiO_2. The most direct way to identify the formation of CH_3CONH_2(a) and CH_3CONH(a) due to CH_3CN adsorption on TiO_2 is to investigate the absorption spectra of CH_3CONH_2 on the surface. Fig. 2 shows the spectra for the adsorbed species after exposing a clean TiO_2 surface to CH_3CONH_2 vapor for 25 min, followed by evacuation at 35 and 175 °C. For the 35 °C spectrum, absorption bands located at 1363, 1410, 1431, 1470, 1552, 1587 and 1654 cm^{-1} are observed. After heating to 175 °C, these bands can be divided into two sets showing opposite trends of intensity

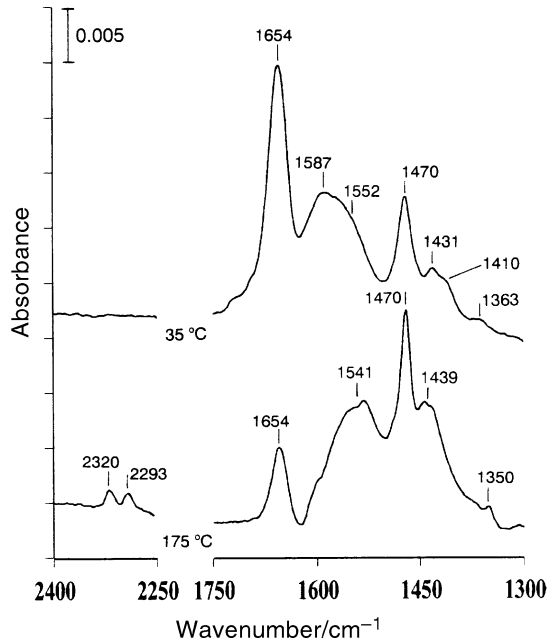

Fig. 2 IR spectra of a TiO_2 surface exposed to the vapor of CH_3CONH_2 for 25 min at 35 °C and then evacuated at 35 °C for 30 min and at 175 °C for 1 min. Both spectra were recorded with 50 scans at 35 °C. The mass of TiO_2 used was ~72 mg.

variation with temperature. One set, including the bands at 1363, 1410, 1587 and 1654 cm^{-1}, decreases in intensity as the TiO_2 temperature is raised. The other set, with bands at 1439, 1470 and 1541 cm^{-1} increases in intensity with increasing temperature. The former set is attributed to adsorbed CH_3CONH_2(a) exhibiting carbonyl stretching at 1654 cm^{-1}, NH_2 bending at 1587 cm^{-1}, C–N stretching at 1410 cm^{-1} and CH_3 bending at 1363 cm^{-1}. This assignment is supported by the similar absorptions of acetamide molecules in liquid as shown in the first column in Table 2. The presence of two sets of bands with opposite intensity change with surface temperature can be explained by the decomposition of acetamide on the surface. A recent study of formamide adsorption on TiO_2 has shown the formation of bridging η^2(N,O)-HCONH(a).[26] A similar dissociation process is expected to occur in the acetamide case. The strong bands at 1439, 1470 and 1541 cm^{-1} in Fig. 2, assignable to –CNO– stretching, reveal the formation of η^2(N,O)-CH_3CONH(a). Acetic acid, analogous to acetamide, is also dissociatively adsorbed on TiO_2 to produce bridging acetate which exhibits strong peaks at 1423 (shoulder), 1456 and 1532 cm^{-1} due to –COO– stretching (this will be shown later in Fig. 4). Comparing the absorption features in the 1250–1750 cm^{-1} region after the adsorption of CH_3CN and CH_3CONH_2 in Fig. 1 and 2, a close resemblance in peak frequency and peak shape is observed. It is concluded that CH_3CN reacts with surface hydroxy groups, generating CH_3CONH_2(a) and η^2(N,O)-CH_3CONH(a) on the surface. Table 2 shows the comparison of the observed frequencies in the 1250–1750 cm^{-1} region after CH_3CN, CD_3CN, CH_3CONH_2 and CH_3COOH adsorption on the TiO_2 surface and the corresponding vibrational mode assignments. In addition to the chemical transformation to CH_3CONH_2(a) and η^2(N,O)-CH_3CONH(a) after acetamide adsorption on TiO_2, new peaks located at 2293 and 2320 cm^{-1} in Fig. 2, which are assignable to CN stretching, grow at temperatures above ~150 °C, indicating that C=O and N–H bonds of the acetamide are thermally activated. These two peaks, together with the 1350 cm^{-1} band are close, in position and relative intensity, to the CH_3CN(a) absorptions at 1367, 2279 and 2308 cm^{-1} in Fig. 1. This similarity suggests the formation of acetonitrile from thermal reorganization of acetamide on TiO_2.

Photochemistry of CH_3CN and CH_3CONH_2

Fig. 3 shows the IR spectra taken before and after the indicated UV irradiation times during the photooxidation of the adsorbed species, which were prepared by exposing a clean TiO_2 surface to CH_3CN vapor and then followed by evacuation, in 10 Torr of O_2. Before UV irradiation, the three species of CH_3CN(a), CH_3CONH_2(a) and η^2(N,O)-CH_3CONH(a) are already known to be present on the surface after CH_3CN adsorption on TiO_2. UV irradiation causes loss or enhancement in intensity for the existing bands and formation of new peaks. After 5 min irradiation, while the amount

Table 2 Vibrational frequencies and assignments of CH_3CONH_2 and η^2(N,O)-CH_3CONH

CH_3CONH_2 liquid (ref. 25)	CH_3CONH_2/ TiO_2 (this work)	Mode description	η^2(N,O)-CH_3CONH/ TiO_2 (this work)	Mode description	η^2(O,O)-CH_3COO/ TiO_2 (this work)	Mode description	CH_3CN/ TiO_2 (this work)	CD_3CN/ TiO_2 (this work)
1660	1654	ν(CO)					1630	1622
1600	1587	$\delta(NH_2)$					1578	
			1541		1532		1537	1518
			1470	ν(CNO)	1456	ν(COO)	1469	1465
			1439		1423		1433	1435
1388	1410	ν(CN)					1415	1416
1345	1363	$\delta(CH_3)$						

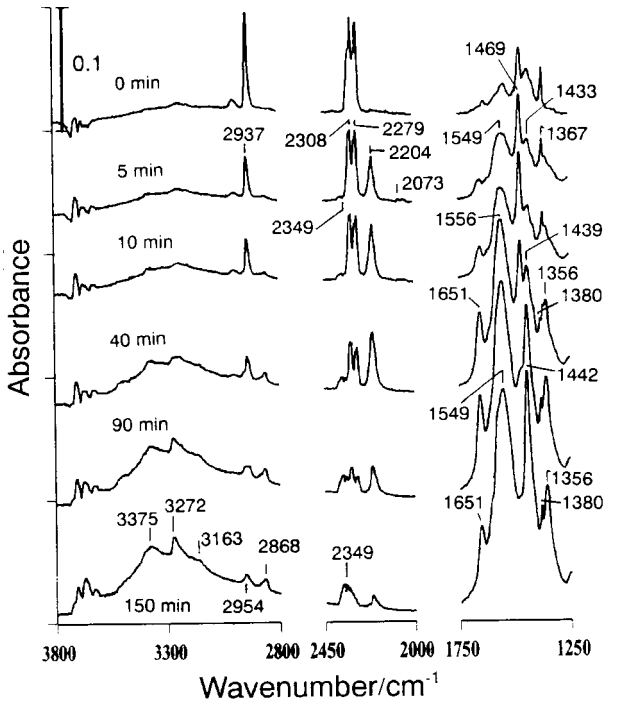

Fig. 3 IR spectra taken before and after the indicated UV exposure times during the photooxidation course of the adsorbed species, which were formed by exposing a clean surface TiO_2 surface to 2 Torr of CH_3CN and then evacuated at 35 °C, in 10 Torr of O_2. Each spectrum was recorded with 5 scans.

of adsorbed CH_3CN decreases, as evidenced by the reduction of its characteristic absorptions at 1367, 2279, 2308 and 2937 cm^{-1}, that of η^2(N,O)-CH_3CONH(a) increases as indicated by the enhancement of the bands at 1433, 1469 and 1549 cm^{-1}. Absorptions of surface OH groups in the 3600–3800 cm^{-1} region increase after irradiation. The observable dip at 2349 cm^{-1} shows the formation of CO_2 in the gas phase. A weak absorption at ~2073 cm^{-1} and a strong band at 2204 cm^{-1} appear. The latter band is identified as adsorbed NCO; a similar band has been observed in the previously studied CH_3CN photooxidation process.[18] The 2073 cm^{-1} band is likely due to the formation of anionic CH_2CN(a) species, as observed in CH_3CN adsorption on a partially oxidized Ag surface,[4] CeO_2,[16] and γ-Al_2O_3[27] with basic surface sites. After 40 min irradiation, CH_3CN(a) continues to decrease. On the other hand, in addition to the increase in CO_2, enhanced absorptions occur at 1356, 1380, 1439, 1556 and 1651 cm^{-1} and in the 3000–3500 cm^{-1} region. After further irradiation to 90 min, CH_3CN(a) and NCO(a) are substantially reduced. The 1469 cm^{-1} band due to η^2(N,O)-CH_3CONH(a) is almost completely depleted. In this photoreaction process, CH_3CN(a) decreases with UV irradiation and is totally consumed after 150 min, in contrast to the monotonic growth of CO_2(g). η^2(N,O)-CH_3CONH(a) increases in the initial stage, however, prolonged irradiation causes its loss. NCO(a) also increases initially with UV irradiation, but gradually declines after 40 min. After 150 min irradiation, the bands left to be identified appear at 1356, 1380, 1442, 1549, 1651, 2868, 2954, 3163, 3272 and 3375 cm^{-1}. The strong absorptions at 1356, 1380, 1442 and 1549 cm^{-1} are attributed to –COO– stretching of acetate and formate formed in the photoreaction. These two species have been identified on metal oxides and in solution at similar frequencies.[28] Previously, in the study of adsorption of formic acid[29] and formaldehyde[30] on TiO_2, HCOO(a) was formed, showing its characteristic absorptions for –COO– stretching at 1360 and 1550 cm^{-1} and for CH deformation at 1380 cm^{-1}. Further confirmation for the formation of acetate on TiO_2 is obtained by examining the absorption frequencies of acetate formed by dissociative acetic acid adsorption on this surface. Fig. 4 shows the IR spectra of the TiO_2 surface after CH_3COOH adsorption followed by evacuation at 35 and 120 °C, respectively. For the spectrum at 35 °C, both CH_3COOH(a) represented by the 1678 cm^{-1} band due to carbonyl stretching, and CH_3COO(a) represented by the 1423, 1452 and 1534 cm^{-1} bands due to –COO– stretching are present on the surface. Heating to 120 °C causes the disappearance of CH_3COOH(a) and increase in CH_3COO(a). The peak positions and relative intensity of the acetate bands at 1456 and 1532 cm^{-1} are similar to those of the growing bands at 1442 and 1549 cm^{-1} in Fig. 3, indicating the formation of acetate groups in the photooxidation of the adsorbed species formed after CH_3CN adsorption on TiO_2. In the photooxidation study of CH_3CN on TiO_2 by Zhuang *et al.*,[18] they also observed similar absorption bands at 1356, 1442 and 1556 cm^{-1} which were assigned to surface carbonate or bicarbonate species. However, in our case, the 1356, 1380, 1442 and 1549 cm^{-1} bands grow with the 2868 and 2954 cm^{-1} bands assignable to CH_x stretching[29,30] in Fig. 3, strongly supporting the formation of formate and acetate during CH_3CN photooxidation in O_2, rather than carbonate or bicarbonate species. In the present study, in addition to formate and acetate formation, the characteristic absorptions at 3163, 3272 and 3375 cm^{-1} in Fig. 3 indicate the formation of species containing NH_x functional groups; these absorption bands, together with that at 1651 cm^{-1}, are found to be very similar to the recent observation in the photooxidation of formamide on TiO_2,[26] suggesting that $HCONH_2$(a) or/and HCONH(a) are likely to be generated. It should be pointed out that the TiO_2 surface temperature was raised to 80 °C upon the UV irradiation in the study for Fig. 3. Therefore a thermal control experiment was carried out by holding the surface temperature at 80 °C for the TiO_2 sample after CH_3CN adsorption and evacuation at 35 °C and by measuring the IR spectra during the surface annealing in 10 Torr of O_2. However, it was found that, after 180 min, as shown in Fig. 5, the major

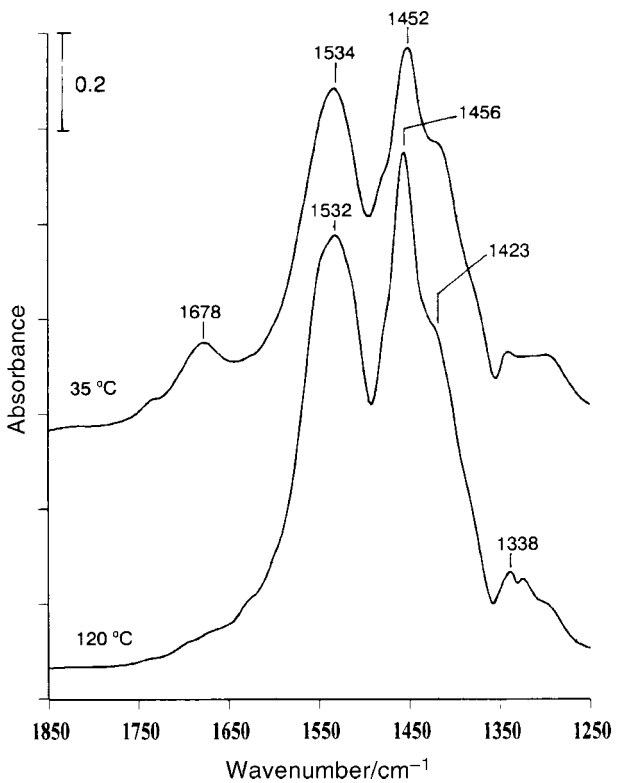

Fig. 4 IR spectra of a TiO_2 surface exposed to 2 Torr of acetic acid and then evacuated at 35 °C for 20 min and at 120 °C for 1 min. Both spectra were recorded with 50 scans at 35 °C. The mass of TiO_2 used was ~67 mg.

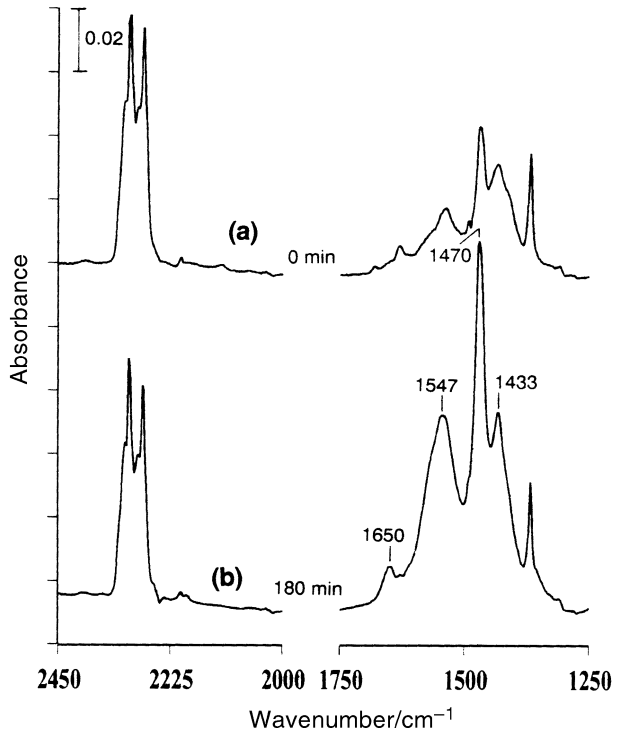

Fig. 5 IR spectra taken after CH_3CN adsorption followed by evacuation at 35 °C (a) and then by 180 min surface annealing at ~80 °C in 10 Torr of O_2 (b).

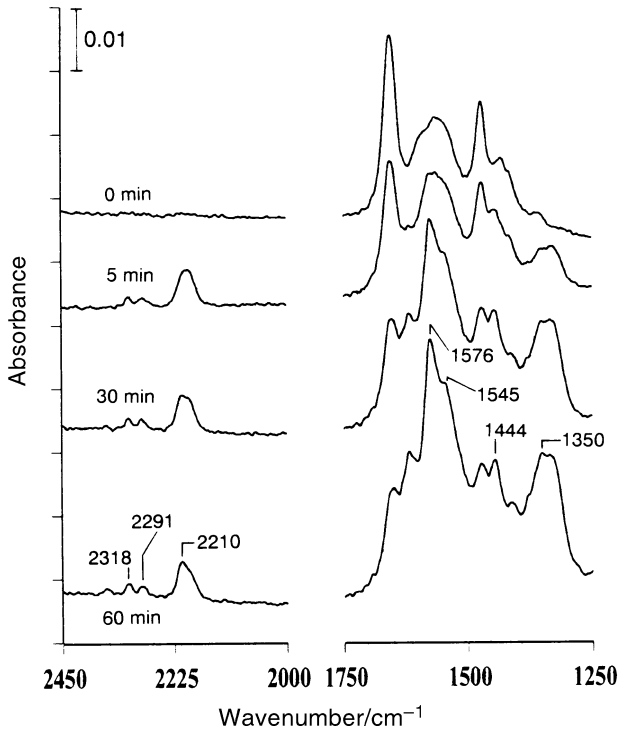

Fig. 6 IR spectra taken before and after the indicated UV irradiation times during the photooxidation process of the adsorbed species, which were formed by exposing a clean TiO_2 surface to CH_3CONH_2 vapor for 25 min followed by annealing at 100 °C for 1 min under vacuum, in 10 Torr of O_2. Each spectrum was recorded with 5 scans.

change of this surface annealing is the enhanced absorptions at 1433, 1470, 1547 and 1650 cm^{-1} due to the increase in adsorbed CH_3CONH_2 and η^2(N,O)-CH_3CONH. Since CH_3CONH_2(a) and η^2(N,O)-CH_3CONH(a) are present on the TiO_2 after CH_3CN adsorption, their photochemistry was also studied. Fig. 6 shows the IR spectra taken before and after the indicated UV times during the photooxidation of the adsorbed species, which were prepared by exposing a clean TiO_2 surface to CH_3CONH_2 followed by evacuation at 100 °C, in 10 Torr of O_2. After UV irradiation, the bands at 1350, 1444, 1545, 1576, 2210, 2291 and 2318 cm^{-1} grow at the expense of CH_3CONH_2(a) and η^2(N,O)-CH_3CONH(a), as evidenced by the decrease in the 1469 and 1654 cm^{-1} bands. Similar positions to the first five growing bands in Fig. 6 are also observed in Fig. 3, indicating the formation of HCOO(a), CH_3COO(a) and NCO(a). The last two new bands at 2291 and 2318 cm^{-1} fall in the CN stretching frequency range, demonstrating the formation of species containing this functional group. A thermal control experiment was also performed to check the surface heating effect during the photoprocess; it showed no formation of the photoreaction bands.

After identification of the species responsible for the observed bands in Fig. 3 and Fig. 6 in the photoreactions catalyzed by TiO_2 after CH_3CN and CH_3CONH_2 adsorption, the reaction pathways following CH_3CN adsorption on TiO_2 are summarized in Scheme 1. CH_3CN(a) is photooxidized to anionic CH_2CN(a) as an intermediate. Adsorbed CH_3CN can react with surface hydroxy groups to form CH_3CONH_2(a) and η^2(N,O)-CH_3CONH(a) which on further photooxidation form HCOO(a), CH_3COO(a), NCO(a) and CN-containing species. In the previous study of CH_3CN photooxidation on TiO_2, Zhuang *et al.*[18] proposed a mechanism for NCO(a) formation directly from CH_3CN adsorbed on a surface Ti ion site. In this mechanism, CH_3N loses the methyl group, forming CO_2(g) and adsorbed CN radical in the photodegradation. NCO(a) results from the CN radical attacking the TiO_2 surface. Since in our study it is found that CH_3CONH_2(a) is generated after CH_3CN adsorption on TiO_2, the reaction pathways shown in Scheme 1 can be viewed to be supplementary to the mechanism provided by Zhuang *et al.*[18] for CH_3CN photooxidation on TiO_2. Because CH_3CN and CH_3CONH_2 do not absorb the UV light used in this study, their photoreaction on TiO_2 must be initiated by TiO_2 bandgap excitation to generate electron–hole pairs. Holes, OH· radicals, and oxygen anionic species are three major species proposed to induce the photooxidation process, however, the exact initiation mechanisms are still under discussion.

In conclusion we demonstrate that CH_3CN can react with surface hydroxy groups on TiO_2 forming CH_3CONH_2(a) and CH_3CONH(a) species, as supported by the same IR absorptions found after CH_3CONH_2 adsorption on the surface. In the photooxidation of CH_3CN, similar to the previous finding,[18] we also observe NCO(a) formation, but together with HCOO(a), CH_3COO(a) *etc.* In addition to the mechanism proposed for NCO(a) formation directly from CH_3CN

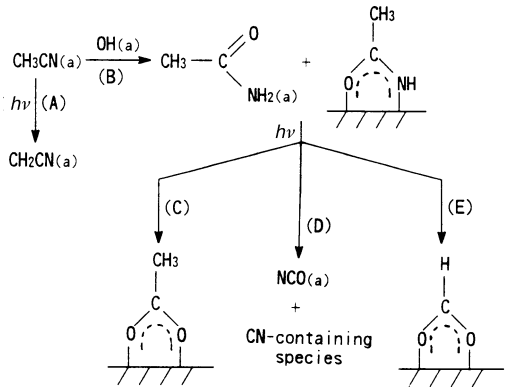

Scheme 1

photodegradation by Zhuang *et al.*[18] we show that these reaction products can result from photooxidation of CH_3CONH_2.

Acknowledgements

We acknowledge financial support from the National Science Council of the Republic of China (NSC 89-2113-M-006-008).

References

1 B. A. Sexton and N. R. Avery, *Surf. Sci.*, 1992, **277**, 123.
2 K. Kishi and S. Ikeda, *Surf. Sci.*, 1981, **107**, 405.
3 C. M. Friend, E. L. Muetterties and J. L. Gland, *J. Phys. Chem.*, 1988, **85**, 3256.
4 A. J. Capote, A. V. Hamza, N. D. S. Canning and R. J. Madix, *Surf. Sci.*, 1986, **175**, 445.
5 C. L. Angell and M. V. Howell, *J. Phys. Chem.*, 1969, **73**, 2551.
6 H. Knözinger and H. Krietenbrink, *J. Chem. Soc., Faraday Trans. 1*, 1975, **71**, 2421.
7 R. E. Sempels and P. G. Rouxhet, *J. Colloid Interface Sci.*, 1976, **55**, 263.
8 P. O. Scokart, F. D. Declerck and R. E. Sempels, *J. Chem. Soc., Faraday Trans. 1*, 1977, **72**, 359.
9 A. G. Pelmenschikov, R. A. van Santen, J. Janchen and E. Meijer, *J. Phys. Chem*, 1995, **97**, 11071.
10 A. Aboulayt, C. Binet and J. C. Lavalley, *J. Chem. Soc., Faraday Trans.*, 1995, **91**, 2913.
11 K. Hagiwara, T. Yamazaki and S. J. Ozawa, *J. Colloid Interface Sci.*, 1995, **170**, 421.
12 J. Szanyi and M. T. Paffett, *J. Chem. Soc., Faraday Trans.*, 1996, **92**, 5165.
13 V. Lorenzelli, G. Busca and N. Sheppard, *J. Catal.*, 1980, **66**, 28.
14 J. C. Lavalley and C. Gain, *C. R. Acad. Sci. Paris Ser. C*, 1979, **288**, 177.
15 H. Krietenbrink and H. Knozinger, *Z. Phys. Chem.* (*Wiesbaden*), 1976, **102**, 43.
16 C. Binet, A. Jadi and J. C. Lavalley, *J. Chem. Phys.*, 1992, **89**, 31.
17 N. N. Lichtin and M. Avudaithai, *Environ. Sci. Technol.*, 1996, **30**, 2014.
18 J. Zhuang, C. N. Rusu and J. T. Yates, Jr., *J. Phys. Chem. B*, 1999, **103**, 6957.
19 P. Basu, T. H. Ballinger and J. T. Yates, Jr., *Rev. Sci. Instrum.*, 1988, **59**, 1321.
20 J. C. S. Wong, A. Linsebigler, G. Lu, J. Fan and J. T. Yates, Jr., *J. Phys. Chem.*, 1995, **99**, 335.
21 Y. Suda, T. Morimoto and M. Nagao, *Langmuir*, 1987, **3**, 99.
22 J. G. Calvert and J. N. Pitts, Jr., *Photochemistry*, Wiley, New York, 1966.
23 E. L. Pace and L. J. Noe, *J. Chem. Phys.*, 1968, **49**, 5317.
24 J. C. Evans and G. Y. S. Lo, *Spectrochim. Acta*, 1965, **21**, 1033.
25 I. Suzuki, *Bull. Chem. Soc. Jpn.*, 1962, **35**, 1279.
26 W.-C. Wu, L.-F. Liao, C.-C. Chuang and J.-L. Lin, *J. Catal.*, in the press.
27 E. Escalona Platero, M. Peñarroya Mentruit and C. Morterra, *Langmuir*, 1999, **15**, 5079.
28 K. Nakamoto, *Infrared and Raman Spectra of Inorganic and Coordination Compounds*, Wiley, New York, 4th edn., pp. 232–233, 1986.
29 C.-C. Chuang, W.-C. Wu, M.-C. Huang, I.-C. Huang and J.-L. Lin, *J. Catal.*, 1999, **185**, 423.
30 G. Busca, J. Lamotte, J.-C. Lavalley and V. Lorenzelli, *J. Am. Chem. Soc.*, 1987, **109**, 5197.